A NEW SEPARATION METHOD FOR GALAXY SPECTRA BASED ON DATA FUSION BETWEEN TWO GRISM ORDERS IN SLITLESS SPECTROSCOPY

Andréa Guerrero, Shahram Hosseini, Yannick Deville, Thierry Contini, Tristan Grégoire

Université de Toulouse, UPS, CNRS, CNES,
IRAP (Institut de Recherche en Astrophysique et Planétologie)
14 av. Edouard Belin, 31400 Toulouse, France

ABSTRACT

We consider the problem of decontaminating galaxy spectra in the context of the EUCLID space mission. The spectra of neighboring astronomical objects being spatially mixed, a source separation method should be used to separate them. Here, we propose a new method based on the fusion of information between first and second-order spectra generated by a grism. Using the optical properties, we propose a regularized criterion and a gradient algorithm to optimize it. The tests using noisy realistic simulated data show that our method leads to better results than a method only based on second-order information.

***Index Terms*—** Source separation, Euclid mission, Data fusion, Slitless spectroscopy, Astronomy

1. INTRODUCTION

This work is developed in the context of the EUCLID space mission [1] that will be launched in 2022 as part of the European Space Agency's program. The purpose is to analyze the spectra of more than 50 million galaxies to better understand the increasing acceleration of the Universe expansion. The detection of emission lines in the galaxy spectra permits to estimate the galaxy redshifts and to understand how dark energy contributes to this acceleration. The EUCLID satellite will observe the sky through a Near-Infrared Spectrometer and Photometer (NISP). The spectrometer is equipped with grisms, which are prisms combined with diffraction gratings, and generates dispersed spectra of incident light. Because of the grating part, several versions of a dispersed spectrum, related to several orders of the diffraction are created by each grism as we can observe in Figure 1. The grism will be optimized so that most of the energy is concentrated in the first-order spectrum, but the zeroth and second-order spectra of bright objects are not negligible. Spectroscopy is usually performed using a slit, allowing light to diffract from only a small region of the sky. However, EUCLID uses slitless spectroscopy such that different orders of each astronomical object spectrum can overlap with the spectra of neighboring objects. An example of such an overlap for two neighboring objects is shown in Figure 2.

This work has been partially funded by CNES (Centre National d'Etudes Spatiales, France)

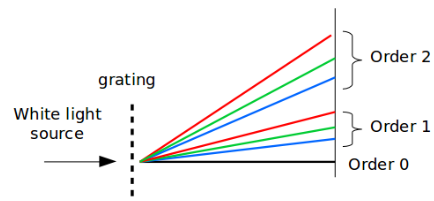

Fig. 1. Orders of spectrum created by grating effect

This contamination of spectra is the main source of redshift estimation errors [2], so a decontamination stage is needed before analyzing each galaxy spectrum, which can be seen as a source separation problem [3], [4]. In [5] we showed that the mixture may be approximated by a linear instantaneous model, and we proposed a method based on Non-negative Matrix Factorization (NMF) [6] to separate it, by only considering the first-order spectra. In this work, we also take into account the second-order, that is optically linked with the first-order (see Section 2). This can be assimilated to a data fusion problem like between panchromatic and hyperspectral images [7] or between multispectral and hyperspectral images [8], [9]. Indeed, using the link between the orders we can improve the spectra decontamination. Thus, we propose a criterion based on this fusion between the two orders and a gradient descent algorithm to minimize it.

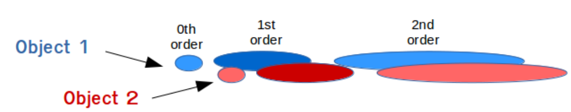

Fig. 2. Mixed dispersed spectra of two neighboring objects at the grism output

2. OPTICAL MODEL AND RESULTING MIXING MODEL

As discussed in [5], the light emitted by each astronomical object is first spatially spread due to its convolution by the instrument Point Spread Function (PSF), then dispersed by a grism. In [5], we assumed that only first-order spectra are important at the grism output. Then, considering that the first-order spectrum of the object of interest is contaminated by the first-order spectra of K-1 contaminating objects, and using some realistic approximations, we showed that the mixing equation can be written as:

$$X = AE + C + B \tag{1}$$

where X is the $M \times N$ observation matrix that contains the observed data, i.e. pixels of the image corresponding to the dispersed light of the object of interest, contaminated by its neighboring objects. A is the $M \times K$ mixing matrix containing the contribution coefficients of each object in each observed pixel, and E is the $K \times N$ source matrix containing in each row the spectrum of each astronomical object up to some indeterminacies explained in [5]. Here we want to decontaminate one object at a time. So, the spectrum of this object of interest we want to estimate is the first row of E, and its contaminating objects are the following rows. C represents the sky background supposedly known that we do not consider in this work because it will be removed in the preprocessing of the EUCLID pipeline. Finally, B is the noise matrix.

As mentioned in Section 1, the grism provides different orders of each spectrum. While the first-order spectrum contains most of light energy, the zeroth and second-orders are non-negligible for bright objects. The zeroth order is basically undispersed and does not contain spectral information, but the second-order contains such an information and it has a better spectral resolution than the first-order, as shown below. Thus, the fusion of information provided by first and second-order spectra should yield a better estimation of the spectral content of the object of interest. The diffraction grating disperses light spatially, and according to [10], [11] and [12] the angular dispersion of each order can be calculated by:

$$\frac{d\theta}{d\lambda} = \frac{m}{a cos\theta} \tag{2}$$

with m the order, λ the wavelength, θ the diffraction angle and a the groove spacing. We take into account the optical geometry resulting from the grating diffraction that we can see in Figure 3: $l = Fo\ tan(\theta)$. where Fo represents the distance between the grism and the focal plane, and l is the diffraction on the focal plane. This yields:

$$\frac{dl}{d\lambda} = Fo \frac{1}{cos^2(\theta)} \frac{d\theta}{d\lambda} = \frac{Fo}{a cos^3(\theta)} m. \tag{3}$$

If we consider a small enough angle θ, which is the case here, then $cos(\theta) \simeq 1$ and this Equation (3) becomes:

$$\frac{dl}{d\lambda} \simeq \frac{Fo}{a} m \quad \Rightarrow \quad l = \frac{Fo}{a} m\lambda + c. \tag{4}$$

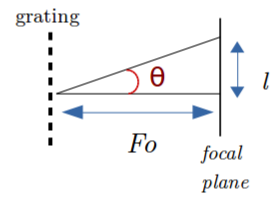

Fig. 3. Optical diagram explaining the dispersion through a diffraction grating

Considering a variation $\Delta\lambda$ of λ, (4) becomes for the first and second-order spectra:

$$\begin{aligned} \Delta l_1 &= \frac{Fo}{a}\Delta\lambda & m = 1 \\ \Delta l_2 &= \frac{Fo}{a} 2\Delta\lambda = 2\Delta l_1 & m = 2 \end{aligned} \tag{5}$$

According to Equation (5), there is a strong link between the first-order spectrum and the second-order one. The latter is twice as dispersed as the first one in the focal plane and its spectral resolution is twice better, such that:

$$s_1(\lambda) = s_2(2\lambda) \tag{6}$$

where s_m are the m-th order source spectra. This redundancy can be used to better estimate the decontaminated spectrum of the object of interest. In practice, we measure discretized spectra so that the following model may be used to link first and second-order spectra:

$$s_1(i) = \frac{s_2(2i-1) + s_2(2i)}{2} \tag{7}$$

where i represents discretized wavelength index.[1] The grism sensitivity varies as a function of wavelength. The measured first and second-order spectra of each object, in the absence of any contaminating object, can be written as

$$e_1(\lambda) = s_1(\lambda) f_1(\lambda) \qquad e_2(\lambda) = s_2(\lambda) f_2(\lambda) \tag{8}$$

where f_1 and f_2 are the grism sensitivity functions respectively for the first and the second-order. The model (1) may be used for each spectral order of the object of interest, i.e.

$$X_1 = A_1E_1 + C + B_1 \qquad X_2 = A_2E_2 + C + B_2 \tag{9}$$

where the first rows of matrices E_1 and E_2 are respectively the row vectors e_1 and e_2 defined in (8) related to the object of interest, and the other rows correspond to contaminating objects of any order. Note that the vector e_2 of size N_2 is twice as large as the vector e_1 of size N_1. Using (6) and (8), we obtain the following link between the two orders

$$\frac{e_1(\lambda)}{f_1(\lambda)} = \frac{e_2(2\lambda)}{f_2(2\lambda)}. \tag{10}$$

To build a separation criterion, we write (10) in a matrix form. For that, we apply the formula described in (7) and get:

$$C_2 e_1^T = C_1 e_2^T. \tag{11}$$

[1] In this paper, we only exploit this link for the object of interest, which must be decontaminated, and not for the contaminating objects.

C_2 and C_1 are respectively $N_1 \times N_1$ and $N_1 \times N_2$ transformation matrices with entries (i, j):

$$C_1(i,j) = \begin{cases} \frac{f_1(i)}{2} & i \le j \le i+1 \\ 0 & otherwise \end{cases} \tag{12}$$

$$C_2(i,j) = \begin{cases} \frac{f_2(2i-1) + f_2(2i)}{2} & i = j \\ 0 & i \neq j \end{cases} \tag{13}$$

These two matrices take into account the dispersion angle difference between the two orders and the grism sensitivity f in each wavelength range. Now that we have established the link between the first and the second-orders, we can build the criterion to decontaminate the source spectra.

3. SEPARATION METHOD BASED ON DATA FUSION BETWEEN TWO ORDERS

3.1. Separation criterion

We propose to minimize the following regularized least-squares criterion:

$$J = \| X_1 - A_1 E_1 \|^2 + \alpha \| X_2 - A_2 E_2 \|^2 + \beta \| C_2 e_1^T - C_1 e_2^T \|^2 \tag{14}$$

where E_m are the estimated source matrices, α and β are real coefficients that we have to fix empirically.

The criterion (14) may be minimized with respect to estimated matrices E_1 (including e_1 in its first row), E_2 (including e_2 in its first row), A_1 and A_2. This can be e.g. done using a modified regularized NMF-based approach which, unfortunately, does not guarantee the unicity of its solution if matrices are initialized randomly. Here, we use a more interesting method for first estimating matrices A_1 and A_2 from direct photometric images, then estimating E_1 and E_2 using a gradient descent algorithm. As explained in [5], the entries of the mixing matrices are related to the object spatial light profiles convolved by the instrument PSF in the cross-dispersion direction. In addition to the spectrometer, the NISP instrument of Euclid is equipped with a three-band photometer which provides direct images of astronomical objects. These images may be used to estimate the position and the shape of each object, then to estimate the mixing matrices A_1 and A_2 from equations provided in [5]. In this work, we used the TIPS simulator [13], developed by the EUCLID consortium, which provides a model of the instrument. So, when the TIPS input is the optical image of an object associated with a constant spectrum, the system output can be used to estimate the columns of the matrices A_1 and A_2 related to that object.

3.2. Gradient descent algorithm

We now use a gradient descent algorithm. Using the properties in [14], we can express the criterion as:

$$\begin{aligned} J = & tr(X_1 X_1^T) + tr(A_1 E_1 E_1^T A_1^T) - 2tr(X_1 E_1^T A_1^T) \\ & + \alpha[tr(X_2 X_2^T) + tr(A_2 E_2 E_2^T A_2^T) - 2tr(X_2 E_2^T A_2^T)] \\ & + \beta(C_2 e_1^T - C_1 e_2^T)^T (C_2 e_1^T - C_1 e_2^T) \end{aligned} \tag{15}$$

with $tr(.)$ the matrix trace. We calculate the gradient of (15) regarding the first-order source matrix:

$$\frac{\partial J}{\partial E_1} = 2A_1^T A_1 E_1 - 2A_1^T X_1 \tag{16}$$

$$+ \beta \frac{\partial (C_2 e_1^T - C_1 e_2^T)^T (C_2 e_1^T - C_1 e_2^T)}{\partial E_1}$$

$$= 2A_1^T A_1 E_1 - 2A_1^T X_1 + \beta \begin{bmatrix} 2(e_1 C_2^T - e_2 C_1^T) C_2 \\ 0 \\ \vdots \end{bmatrix}. \tag{17}$$

For the gradient regarding E_2, we have:

$$\frac{\partial J}{\partial E_2} = 2\alpha A_2^T A_2 E_2 - 2\alpha A_2^T X_2 - \beta \begin{bmatrix} 2(e_1 C_2^T - e_2 C_1^T) C_1 \\ 0 \\ \vdots \end{bmatrix}. \tag{18}$$

Matrices E_1 and E_2 are initialized to random values, then updated using this update rule until convergence:

$$E_m \leftarrow E_m - \mu \frac{dJ}{dE_m} \tag{19}$$

where μ is a small positive gradient step.

4. TESTS AND RESULTS

To test our method, we simulate observed data with the TIPS simulator mentioned in Section 3.1: we put two optical images of two neighboring astronomical objects and their spectra at its input and we obtain the mixture at its output. One of the objects is considered as the object of interest and the other one as the contaminating object. We aim in estimating the decontaminated second-order spectrum of the object of interest, which has a better resolution than the first-order spectrum, but is fainter. To analyze the robustness of our

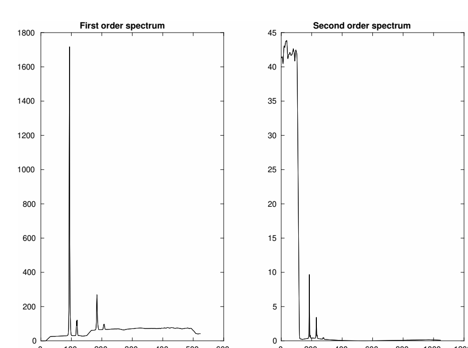

Fig. 4. Mixed noiseless spectra

method to noise, we add realistic noise (taking into account the sky background) to the mixture, and evaluate the performance for different Signal-to-Noise Ratio (SNR), defined by: $SNR = 10log_{10}(\frac{P_s}{P_b})$ with P_s the actual second-order spectrum power of the object of interest and P_b the noise power. The mixed noiseless first and second-order spectra are shown in Fig. 4. In the first-order spectrum, the first two emission lines belong to the object of interest, while the last two lines belong to the contaminating object. The leftmost part of the second-order spectrum is contaminated by the continuum of the first-order spectrum of the contaminating object. To quantify the estimation quality, we use the following performance criterion called the Normalized Root-Mean-Square Error (NRMSE):

$$NRMSE_m = \sqrt{\frac{norm(s_m - \widehat{s}_m)^2}{norm(s_m)^2}} \tag{20}$$

where s_m is the true $m^{th}-$order spectrum of the object of interest and $\widehat{s}_m$ its estimate. We empirically fix the gradient step μ to 0.3 to ensure the algorithm convergence. The two parameters α and β defining the importance of each term in the separation criterion (14) must be set up. Their optimal values depend on the SNR. When the SNR is high, the second-order spectrum is not very noisy and the second term in the criterion (14) is almost enough to achieve a good estimation. So, we should use a large value for α and a much smaller value for β. When the SNR is low, the second-order spectrum is very noisy such that the second term in the criterion is less important: we have to reduce its weight, α, and increase the weight of the third term, β, since this term links the second-order spectrum to the first-order one which is much less noisier.

Table 1 shows the NRMSE obtained for the first and the second-order estimated spectra as a function of the parameter setting, for relatively low values of SNR of the simulated mixture. We also tested the estimation of the second-order spectrum only based on the second-order information, where we only keep the second term of the criterion (14). In Table 1, we see that the whole criterion provides a better estimation of the second-order spectrum especially for lower SNR in comparison with the estimation obtained by keeping only the second term in our criterion. The actual second-order spectrum of the object of interest is shown in Fig. 5 and its estimates using only the second term in the criterion and using the whole criterion are shown in Fig. 6 for an SNR of 30dB. We can see that the whole criterion provides a significant improvement, especially for the second emission line in the true spectrum.

SNR (dB)	α	β	$NRMSE_1$	$NRMSE_2$	$NRMSE_2$ term 2 only
30	1e-8	1e-3	0.04	0.43	0.75
25	1.8e-8	1e-4	0.04	0.43	1.01
12	1.1e-8	1e-4	0.06	0.44	1.32
7	8e-9	1e-4	0.09	0.48	1.37

Table 1. NRMSE evolution as a function of SNR value

From Table 1, we also notice that the first-order spectrum is always well estimated because it is less noisy.

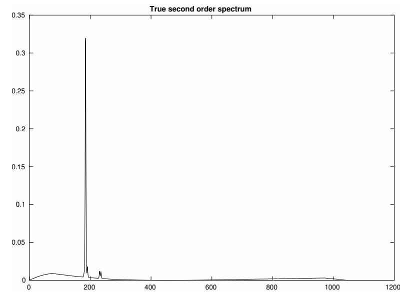

Fig. 5. True second-order spectrum

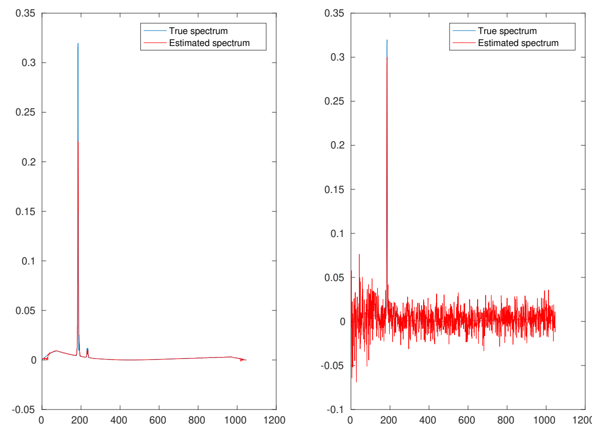

Fig. 6. True second-order spectrum (blue) and its estimations (red) using only the second term in the criterion (at the right) and using the whole criterion (at the left) for $SNR = 30dB$.

5. CONCLUSION

In this work, we presented a new decontamination method adapted to the EUCLID data, based on the fusion between information from the first and the second orders. We showed that adding the first and second order link in the separation criterion improves the estimation of the second-order spectrum of the object which should be decontaminated. Here, we estimated the mixing matrices thanks to optical images from another EUCLID instrument. However, the astronomical object positions are only approximately known, so in future work, we want to allow these mixing matrices to be adjusted during the spectra estimation. For that, a semi-blind algorithm should be considered. Also, we only used information provided by one grism, but in the EUCLID satellite there will be 3 grisms with different orientations. The fusion of information provided by the 3 grisms will improve the spectra decontamination. Finally, our method has been applied to the Euclid simulated data, but it can also be used in other applications where grating diffraction is used for spectroscopy.

Acknowledgement
The authors would like to thank N. Fourmanoit and J.-P. Pérez for helpful discussions.

6. REFERENCES

[1] "Euclid consortium page," https://www.euclid-ec.org/, 2018.

[2] "Euclid Definition Study Report," https://arxiv.org/pdf/1110.3193.pdf, 2011.

[3] P. Comon and C. Jutten, *Handbook of Blind Source Separation. Independent Component Analysis and Applications*, Academic Press, 2010.

[4] Y. Deville, "Blind source separation and blind mixture identification methods," in *Wiley Encyclopedia of Electrical and Electronics Engineering*, pp. 1–33. J. Webster, 2016.

[5] A. Selloum, S. Hosseini, Y. Deville, and T. Contini, "Mixing model in slitless spectroscopy and resulting blind methods for separating galaxy spectra," in *Machine Learning for Signal Processing (MLSP 2016)*, Salerno, Italy, September 2016.

[6] Andrzej Cichocki, Rafal Zdunek, Anh-Huy Phan, and Shun-ichi Amari, *Nonnegative Matrix and Tensor Factorizations: Applications to Exploratory Multi-Way Data Analysis and Blind Source Separation*, 10 2009.

[7] L. Loncan, et al., "Hyperspectral pansharpening: a review," *IEEE Geoscience and Remote Sensing Magazine*, vol. 3, pp. 27–46, Sep 2015.

[8] M. S. Karoui, Y. Deville, F. Z. Benhalouche, and I. Boukerch, "Hypersharpening by joint-criterion nonnegative matrix factorization," *IEEE Transactions on Geoscience and Remote Sensing*, vol. 55, no. 3, pp. 1660–1670, March 2017.

[9] N. Yokoya, T. Yairi, and A. Iwasaki, "Coupled nonnegative matrix factorization unmixing for hyperspectral and multispectral data fusion," *IEEE Transactions on Geoscience and Remote Sensing*, vol. 50, no. 2, pp. 528–537, Feb 2012.

[10] M. Born and E. Wolf, *Principles of Optics: Electromagnetic Theory of Propagation, Interference and Diffraction of Light*, Pergamon Press, 1970.

[11] C. Palmer and E. Loewen, *Diffraction grating handbook*, Richardson Gratings, 2014.

[12] J.P. Pérez, *Optique - Fondements et applications*, Dunod, 2004.

[13] "TIPS simulator," http://projects.lam.fr/projects/tips/wiki.

[14] K. B. Petersen and M. S. Pedersen, *The Matrix Cookbook*, Technical University of Denmark, Nov. 2012.